Chemical Engineering Journal 154 (2009) 9–16

Contents lists available at ScienceDirect

Chemical Engineering Journal

journal homepage: www.elsevier.com/locate/cej

A study on thermal combustion of lean methane–air mixtures: Simplified reaction mechanism and kinetic equations

Krzysztof Gosiewski*, Anna Pawlaczyk, Krzysztof Warmuzinski, Manfred Jaschik

Institute of Chemical Engineering, Polish Academy of Sciences, ul. Baltycka 5, 44-100 Gliwice, Poland

ARTICLE INFO

Article history:
Received 25 November 2008
Received in revised form 2 February 2009
Accepted 16 March 2009

Keywords:
Chemical reactors
Homogeneous methane combustion
Kinetics
Reaction mechanism
Monolith packing
Mine ventilation air

ABSTRACT

Homogeneous combustion of lean methane–air mixtures occurs in both thermal and catalytic reverse-flow reactors. The modeling and design of such reactor requires a reliable and relatively simple kinetic model of the combustion. Although a number of detailed descriptions of the kinetics of homogeneous combustion are available in the literature (including those which take into account complex free-radical reactions), their practical usefulness is doubtful. In the present study a simple one- or two-stage model is proposed which directly describes global kinetics and neglects intermediates and radicals. Special attention is paid to the mechanism of the possible formation of carbon monoxide. The studies were done both for the combustion in the free space and for the process taking place over a monolith packing.

1. Introduction

The combustion of lean methane–air mixtures combined with the recovery of the heat of reaction is an important problem for the mining industry, as methane concentration in mine ventilation air is usually below 1 vol.%. Since the flowrates of this air from a single ventilation shaft usually exceed 500,000 m^3/h, the methane gas should be somehow utilized rather than released into the atmosphere. One of the most reasonable options seems to be the combustion of CH_4 in reverse-flow reactors with the simultaneous heat recovery. Both catalytic (CFRR) and non-catalytic (thermal) flow-reversal reactors (TFRR) are intensively studied. In both types of reactors homogeneous combustion occurs partially (in CFRR) or totally (in TFRR) in the gas phase. Therefore, the knowledge of the mechanism and kinetics of the combustion is crucial in the design and simulation studies.

The results presented in the present paper include combustion both in the free space and over a monolith. Conclusions are also proposed concerning a simplified description of the mechanism and kinetics of the process.

2. An overview of the combustion mechanisms for low molecular weight hydrocarbons

The processes of combustion are usually associated with a multitude of reactions with complex kinetics and, often, strongly influenced by mass transfer and fluid flow phenomena. An extensive literature survey did not yield any unique kinetic mechanism for the homogeneous combustion of methane. The chemical reactions themselves may be discussed using various levels of detail. The oxidation of methane is obviously a free-radical process that may include several (to several hundred) consecutive elementary reactions (see, e.g., the complex scheme of a multi-stage reaction proposed in Ref. [1]). Free radicals which may form during the oxidation and the principal directions of the process producing stable products (e.g., carbon oxide or dioxide) can be generally described as a series of consecutive reactions [2]. Some of the detailed mechanisms based on numerical simulations are presented in Table 1 (the table is taken from Ref. [3]). The numbers quoted in this table lead to a question about the most realistic mechanism. Highly detailed and complex combustion mechanisms obtained by several authors using numerical simulations may differ widely. Moreover, the guidelines are missing that would suggest which of the published complex models should be employed in a given case. Therefore, we have to find a compromise between simple, one-step models and multi-stage models based on a large number of reactions. Such a compromise approach should yield reliable values of the combustion temperature and concentrations of the main species, and also predict the ignition and extinction conditions. Additionally the model should contain a limited number of reactions that would be easy to validate experimentally, and should correctly predict the formation of the reaction products [4].

Consequently, alongside these complex kinetic models attempts have been made to describe homogeneous combustion using a simplified single-step (or containing less than ten steps, at

* Corresponding author. Tel.: +4832 2310811x126; fax: +4832 2310318.
E-mail address: k.gosiewski@iich.gliwice.pl (K. Gosiewski).

1385-8947/$ – see front matter © 2009 Elsevier B.V. All rights reserved.
doi:10.1016/j.cej.2009.03.045

Nomenclature

a, b, c	exponents at methane concentration in the kinetic equation
C_i	concentration of component i (mol m^{-3})
$C_{p,k}^{calc}$	concentration of reaction product calculated from kinetic equation for the k-th experiment (mol m^{-3})
$C_{p,k}^{meas}$	concentration of reaction product in the k-th experiment (mol m^{-3})
E_j^{con}	activation energy in the j-th kinetic equation for the consecutive scheme (kJ mol^{-1})
E_j^{par}	activation energy in the j-th kinetic equation for the parallel scheme (kJ mol^{-1})
k_j^{con}	reaction rate constant in the j-th kinetic equation for the consecutive scheme (mol$^{(1-a)}$ m$^{-3(1-a)}$ s^{-1})
$k_{j,0}^{con}$	pre-exponential factor in the j-th kinetic equation for the consecutive scheme (mol$^{(1-a)}$ m$^{-3(1-a)}$ s^{-1})
k_j^{par}	reaction rate constant in the j-th kinetic equation for the parallel scheme (mol$^{(1-a)}$ m$^{-3(1-a)}$ s^{-1})
$k_{j,0}^{par}$	pre-exponential factor in the j-th kinetic equation for the parallel scheme (mol$^{(1-a)}$ m$^{-3(1-a)}$ s^{-1})
k_0	pre-exponential factor in kinetic equation (mol$^{(1-a)}$ m$^{-3(1-a)}$ s^{-1})
L_{comb}	length of the combustion zone (cm)
n	number of experimental points used in the estimation of kinetics
R	gas constant (kJ mol^{-1} K^{-1})
r_k^{meas}	reaction rate measured experimentally in the k-th experiment (mol m^{-3} s^{-1})
r_k^{calc}	reaction rate calculated from kinetic equation for the k-th experiment (mol m^{-3} s^{-1})
t	time (s)
T	temperature (K) or (°C)
T_{av}	average temperature in the reaction zone of the monolith (K) or (°C)
T_{ign}	ignition temperature (K) or (°C)

Greek symbols

α_{CH_4}	average total conversion of methane (%)
$\alpha_{CH_4/CO}$	average total conversion of methane to carbon monoxide (%)
α_{CH_4/CO_2}	average total conversion of methane to carbon dioxide (%)
Δ_r	average relative error (Eq. (9)) for the reaction rate (%)
Δ_c	average relative error (Eq. (10)) for the outlet concentration (%)

most) model of the process. Furthermore, it is difficult to assess the agreement between the equations proposed and the actual processes occurring during the combustion of methane under different conditions. The initial attempts at describing the kinetics of the combustion were less than satisfactory. In further studies, mechanisms were approximated using a single equation (or several equations at most). Selected simplified kinetic models for methane combustion, taken from the relevant literature are shown in Table 2. The kinetic parameters, E and k_o, quoted in the table pertain only to this reaction in which CH_4 reacts directly with oxygen.

Table 1
Comparison of the detailed mechanisms of methane oxidation [3].

Source	Species	Number of reactions
Warnatz [8]	29	123
Tsang [9,10]	27	371
Dagaut et al. [11]	31	395
Smith et al. [12]	30	350
Mackie [13]	31	294
Hunter et al. [14]	40	411
Ranzi et al. [4]	44	642
Barbe et al. [3]	42	835

3. Assumption used in the present study

The principal assumption made in developing a mathematical description of the homogeneous combustion of methane is that the model should be useful in simulating processes in large-scale reverse-flow reactors. The model can be subject to the accumulation of numerical errors resulting from periodic changes in initial conditions that reflect flow reversal. Consequently, any errors incurred over a given half-cycle are "recycled" with the initial conditions for the subsequent half-cycles. The attainment of a cyclic steady state may require the simulation of as many as several hundred half-cycles of flow reversal. A sufficiently accurate description of the steady state thus necessitates the use of sophisticated numerical methods. It would thus be unreasonable to complicate further the model by the inclusion of the numerically cumbersome multi-stage kinetics based on excessive number of chemical reactions. Moreover, we have to remember that each new intermediate species that appears in the kinetic formulations requires an additional differential balance equation. Consequently, several tens of components (cf. e.g., the number of species in Table 1) mean additional tens of nonlinear differential equations. It is therefore assumed that the kinetics should be based upon a simple single-step scheme leading directly to CO_2 and H_2O as the sole products or, at most, on a two-stage mechanism with CO as the only intermediate product. This approach is corroborated experimentally as the stable combustion products included only CO, CO_2 and H_2O; no other species (e.g., hydrogen) were experimentally detected. The absence of hydrogen in the combustion products was also mentioned in [5].

Both the combustion mechanism and the kinetic parameters of simplified models may strongly depend on the environment in which the oxidation occurs. This is suggested by the comparison of simulation results for several selected kinetic models (cf. [6]), as well as by the view prevailing among those dealing with homogeneous combustion. The most plausible explanation is that, depending on the size and nature of the surface in contact with gaseous phase, the degree of activation of free radicals may vary. The large surface area of the monolith channels may have a significant effect on the type of combustion products by activating and deactivating radicals in redox processes. Therefore, the studies were conducted in both free space and over Monoliths A and B. The initial studies over granular bed and Monolith A [7] assumed a simple single-stage combustion scheme leading to CO_2

$$CH_4 + 2O_2 \rightarrow CO_2 + 2H_2O \quad (1)$$

In further studies on simplified models the following reactions were also taken into account; these reactions include carbon monoxide as an intermediate species and may follow either consecutive or parallel paths:

$$2CH_4 + 3O_2 \rightarrow 2CO + 4H_2O \quad (2)$$

$$2CO + O_2 \rightarrow 2CO_2 \quad (3)$$

Table 2
Selected simplified reaction mechanisms available in the literature.

Ref.	Number of stages	E	k_o	Application
[15]	1	130,000	2.6×10^8	Lean combustion in porous
	1		4.0×10^{20}	
[16]	2	318,197	1.0×10^{21} and 5.0×10^{16}	Turbulent premixed
	3		6.7×10^{18}	
[17]	3	490,554	16×10^{18}	Partial oxidation in inert
[18]	1	130,038	7.74×10^8	Methane diffusion flame
[5]	2	427,064	1.24×10^{21}	Combustion on small-diameter ceramic tubes
	1	202,641	1.3×10^8	
[19]	2	202,641	2.8×10^9	Numerical laminar flame model
	1 global + 21 elementary reactions	202,641	4×10^9	
[20,21]	1	130,628	1.92×10^{18}	Premixed, laminar, steady-state flames
[2]	1	Not available	Not available	Not available
[22]	4	Not available	Not available	Numerical description of hydrocarbon flames

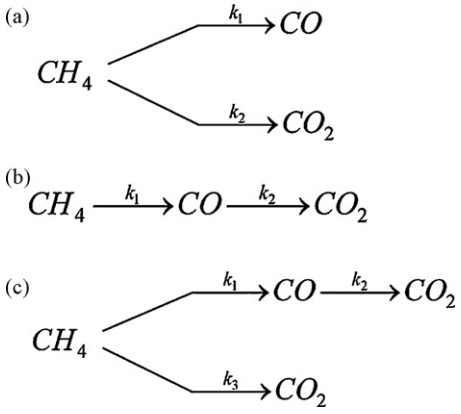

Fig. 1. Reaction mechanisms studied for the homogeneous combustion of methane: (a) parallel, (b) consecutive, (c) consecutive–parallel.

During the combustion over the monolith (termed Monolith A) CO was totally absent from the product mixture. However, there were serious hints that, temporarily, considerable amounts of carbon monoxide can appear in the products. The studies reported in Ref. [5] were carried out only in an empty reactor. Therefore special attention was paid to the conditions under which CO might appear over monoliths, and to the resulting form of a kinetics model. Further studies were thus conducted for both free-space combustion and for a monolith with wider channels (Monolith B).

For Monolith A, due to the absence of CO in the products a simple, single-step combustion mechanism was assumed (reaction (1)). On the other hand, the experimental results obtained in the free-space system and in Monolith B were interpreted by estimating the error (Eq. (9)) incurred in the evaluation of the reaction rate, r_i^{calc}. This rate was calculated for three different reaction mechanisms (cf. Fig. 1), based on the arbitrarily assumed forms of kinetic equations (Eqs. (4)–(8)).

Due to the large excess of oxygen, the kinetic equations for the three mechanisms do not have to include oxygen concentration. Therefore, these equations can be written as follows:

for the parallel mechanism

$$-\frac{dC_{CH_4}}{dt} = k_1^{\text{par}} C_{CH_4}^a = k_{1,0}^{\text{par}} \exp\left(\frac{-E_1^{\text{par}}}{RT}\right) C_{CH_4}^a \quad (4)$$

$$-\frac{dC_{CH_4}}{dt} = k_2^{\text{par}} C_{CH_4}^b = k_{2,0}^{\text{par}} \exp\left(\frac{-E_2^{\text{par}}}{RT}\right) C_{CH_4}^b \quad (5)$$

for the consecutive mechanism

$$-\frac{dC_{CH_4}}{dt} = k_1^{\text{con}} C_{CH_4}^a = k_{1,0}^{\text{con}} \exp\left(\frac{-E_1^{\text{con}}}{RT}\right) C_{CH_4}^a \quad (6)$$

$$-\frac{dC_{CO}}{dt} = k_2^{\text{con}} C_{CO}^b = k_{2,0}^{\text{con}} \exp\left(\frac{-E_2^{\text{con}}}{RT}\right) C_{CO}^b \quad (7)$$

For the consecutive–parallel scheme, which is a combination of the other two mechanisms, the corresponding equation can be written by supplementing the equations for the consecutive mechanism (Eqs. (6) and (7)) with a formula describing the parallel *single-step* combustion of methane:

$$-\frac{dC_{CH_4}}{dt} = k_3^{\text{par}} C_{CH_4}^c = k_{3,0}^{\text{par}} \exp\left(\frac{-E_3^{\text{par}}}{RT}\right) C_{CH_4}^c \quad (8)$$

4. Combustion in the free space

Previous studies carried out in the pelletized bed and in Monolith A were extended onto combustion in a free space. These studies were done in an empty cylindrical reactor 10 mm × 210 mm (shown schematically in Fig. 2), over a temperature range of 500–890 °C and for methane concentrations from 0.5 to 1.4 vol.%; the flow rate of the feed gas was kept at 120 l/h. The supply of the reactants to the reaction zone and their withdrawal from the system was affected by

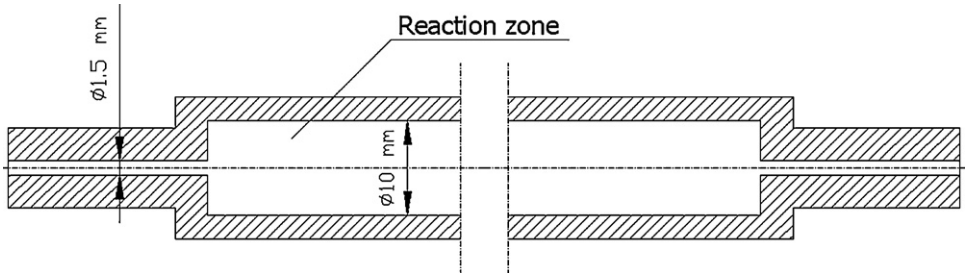

Fig. 2. Combustion chamber for the oxidation in the free space.

Table 3
The estimated values of the kinetic parameters.

Reaction system (ignition temperature)	Reaction mechanism		Reaction	E [J mol^{-1}]	k_o [mol$^{(1-a)}$ m$^{-3(1-a)}$ s^{-1}]	a, b, c	Error Eq. (9) [%]	Error Eq. (10) [%]
Free space ($T_{ign} \approx 830\,^{\circ}C$)	Two-stage	Parallel	$2CH_4 + 3O_2 \xrightarrow{k_1} 2CO + 4H_2O$	222,647	2.99×10^{10}	1	6.24	5.31
			$CH_4 + 2O_2 \xrightarrow{k_2} CO_2 + 2H_2O$	1125,422	1.52×10^{52}	1	26.53	7.51
		Consecutive	$2CH_4 + 3O_2 \xrightarrow{k_1} 2CO + 4H_2O$	349,189	7.59×10^{16}	1.5	9.96	13.38
			$2CO + O_2 \xrightarrow{k_2} 2CO_2$	571,532	1.05×10^{27}	1.7	14.66	2.91
	Three-stage	Consecutive–parallel	$2CH_4 + 3O_2 \xrightarrow{k_1} 2CO + 4H_2O$	290,651	8.74×10^{13}	1.4	9.37	11.24
			$2CO + O_2 \xrightarrow{k_2} 2CO_2$	527,101	1.31×10^{25}	2.2	14.89	2.35
			$CH_4 + 2O_2 \xrightarrow{k_3} CO_2 + 2H_2O$	999,074	3.85×10^{47}	1	23.51	2.10
Monolith A ($T_{ign} \approx 530\,^{\circ}C$)	Single-stage		$CH_4 + 2O_2 \xrightarrow{k} CO_2 + 2H_2O$	130,622	6.86×10^{6}	0.94	6.10	0.9
	Two-stage	Parallel	$2CH_4 + 3O_2 \xrightarrow{k_1} 2CO + 4H_2O$	79,904	2.84×10^{2}	1	9.38	0.91
			$CH_4 + 2O_2 \xrightarrow{k_2} CO_2 + 2H_2O$	260,304	8.71×10^{11}	1	15.76	1.41
Monolith B ($T_{ign} \approx 675\,^{\circ}C$)		Consecutive	$2CH_4 + 3O_2 \xrightarrow{k_1} 2CO + 4H_2O$	112,996	2.52×10^{4}	0.9	20.88	2.35
			$2CO + O_2 \xrightarrow{k_2} 2CO_2$	137,388	2.95×10^{6}	1.1	13.78	7.5
	Three-stage	Consecutive–parallel	$2CH_4 + 3O_2 \xrightarrow{k_1} 2CO + 4H_2O$	127,734	1.08×10^{5}	0.8	9.67	0.42
			$2CO + O_2 \xrightarrow{k_2} 2CO_2$	170,952	7.61×10^{7}	1	13.27	3.38
			$CH_4 + 2O_2 \xrightarrow{k_3} CO_2 + 2H_2O$	306,927	5.38×10^{13}	0.7	18.60	0.27

tubes of small diameters. At a suitably selected value of the flow rate the considerable difference in linear velocities in transport tubes (18.9 m/s) and those in the reaction zone (0.42 m/s) exclude the combustion in the transport conduits, limiting this process to the reaction zone itself. The study corroborates earlier results obtained elsewhere [5], namely that the combustion in the free space, over certain temperature ranges, occurs with the production of considerable amounts of carbon monoxide, and only at higher temperatures does it lead to carbon dioxide. It can therefore be assumed that the oxidation of methane in this system is a consecutive reaction. A comparison between methane combustion in the free space and the same process over a monolith reveals that the ignition temperatures for the mixture methane–air differ considerably. This temperature is about 155–300 °C higher for the combustion in the free space (around 830 °C for the free-space oxidation 530 °C for Monolith A and 675 °C for Monolith B). Furthermore, whereas the monolith combustion is a fairly stable process, the free-space oxidation is unstable and the results may be difficult to reproduce.

During the combustion in the free space methane was oxidized to carbon dioxide and carbon monoxide, with the conversion degree to CO as high as 43%. Roughly, the results agree with those obtained elsewhere (Ref. [5]) where the combustion occurred over a similar range of temperatures. It is interesting, however, to note that the results reported in [5] reveal a visible shift of CO_2 formation towards higher temperatures. This shift may suggest a clear domination of the consecutive mechanism or even (as assumed in [5]) the sole existence of this particular mechanism. However, such a shift is hardly visible in Fig. 3.

This may be due to a simultaneous contribution of a parallel mechanism, or even its dominance. Therefore, the kinetic constants were determined separately for the three mechanisms. The kinetic parameters thus evaluated for both free-space combustion and oxidation over Monoliths A and B are shown in Table 3.

Examples of the experimental Arrhenius plots for the estimation of parameters of Eqs. (6) and (7) are shown in Figs. 4 and 5.

The ignition temperature for lean CH_4–air mixtures (below 1 vol.% of CH_4) was about 825–830 °C; this may be seen in a graph illustrating the conversion of methane as a function of temperature—Fig. 6.

The analysis of the values of kinetic parameters (activation energy and pre-exponential factor), for the combustion in the free space and for both the parallel and the consecutive–parallel schemes reveals that these values become physically meaningless especially for the reaction (1), of oxidation of CH_4 to CO_2.

Excessively large values of E and k_o yield, upon insertion into the relevant kinetic equation, the result close to indeterminate form ($\infty \times 0$). Since the usefulness of such a model is doubtful, it is better to assume that the combustion of methane in the free space

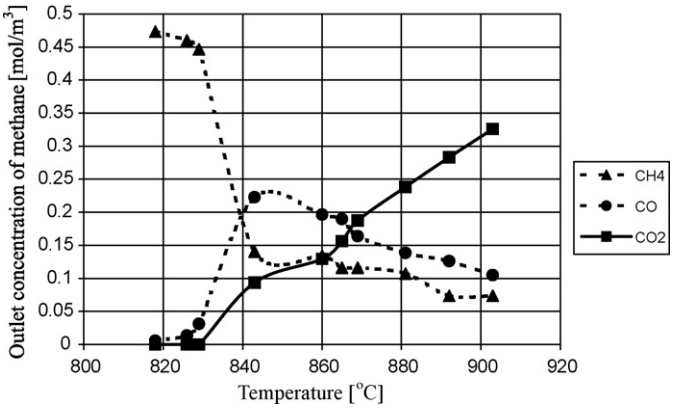

Fig. 3. Outlet concentration profiles vs. temperature for an empty reactor.

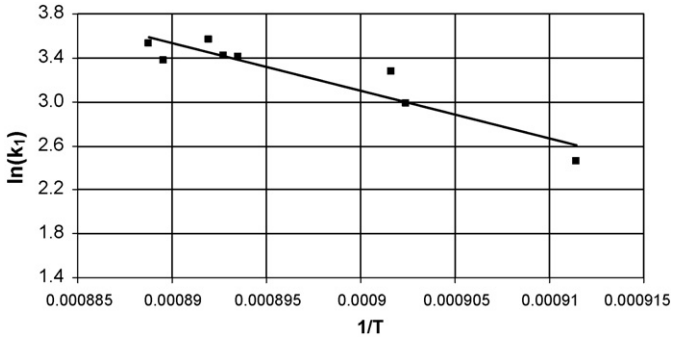

Fig. 4. The Arrhenius plot for the consecutive scheme—combustion of methane to carbon monoxide.

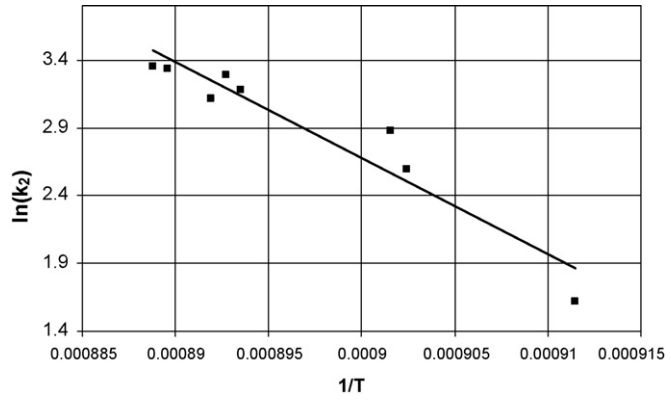

Fig. 5. The Arrhenius plot for the consecutive scheme—combustion of carbon monoxide to carbon dioxide.

occurs according to a simplified scheme of consecutive reactions. Also, the consecutive–parallel scheme suggests that carbon dioxide occurring during the combustion in the free space is a product of the consecutive oxidation of CO rather than a direct result of CH_4 oxidation. This is further supported by a very high values of the activation energy and the pre-exponential factor for reaction (1), for both parallel and consecutive–parallel schemes. However, for the oxidation of methane to CO (reaction (2)) the values of k_o and E estimated based on data presented in Ref. [5] for the consecutive mechanism and the oxidation in the free space would be as follows: $k_1^{con} = 1.24 \times 10^{21}$ (l/s) and $E_1^{con} = 427,065$ (J mol^{-1}), that is, would be close to the values shown in Table 3.

The foregoing discussion shows that, for the combustion in the free space, it is the consecutive mechanism, which should be assumed as a more reliable basis for the kinetic description.

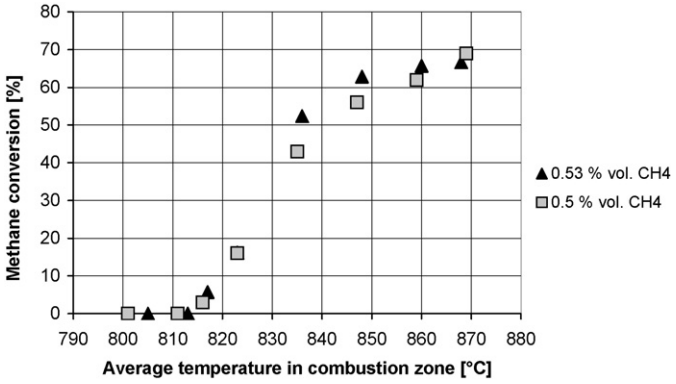

Fig. 6. Conversion degree of methane vs. temperature for inlet concentrations of CH_4 of 0.53 and 0.5 vol.% (combustion in the free space).

Table 4
Parameters of the monolith packing.

Quantity	Unit	Monolith A	Monolith B
Diameter	cm	3.9	6.5
Length*	cm	40 (4 × 10)	120 (4 × 30)
Channel width	mm	2	3
Wall thickness	mm	0.5	0.7
Open frontal area (OFA)	%	64	66
Geometric surface area (GSA)	m^2/m^3	1200	870
Channels per square inch (CPSI)	1/in.^{2}	~100	~50

* *Note*: The total length of the monolith is not the same as the combustion zone (hot zone), which was determined separately for each experiment.

5. Combustion over the monoliths

The experiments were done for two types of Monoliths A and B (cf. Table 4 and Fig. 7).

Kinetic experiments were carried out in a ceramic tube, packed in the middle section with monolith segments. The tube was placed in a temperature-controlled oven. The photographs (Fig. 8) show the experimental installation and the positioning of the monolith sections in the reactor tube.

The results for Monolith A were already presented in Ref. [7]. It has to be stressed that, since no CO was detected during the combustion on this monolith, the relevant kinetics could be described by a simple single-stage mechanism.

Kinetic experiments over Monolith B were conducted in a ceramic tubular reactor of a diameter of 65 mm, symmetrically placed in an oven and packed with three monolith sections of a total length of 900 mm. The experimental setup and the positioning of the monolith sections are shown in Fig. 8. The experiments were carried out over the range of temperatures from 660 to 820 °C and for the inlet methane concentrations between 0.38 and 1.2 vol.%; the flow rate was 0.8 m^3(STP)/h.

Similarly as in [7], the length and volume of the combustion zone were determined based on this section of the temperature profile along the monolith for which the temperature exceeded the ignition temperature. The temperature inside the reactor was measured with thermocouples (1.5 mm in diameters) located close to the axis of the reactor. To avoid placing too many thermocouples in the monolith channels it is assumed that, for a given cross-section, the temperature remains constant along the radius of the reactor. The determination of the combustion temperature was done in the following way. Since the total length of the monolith was larger than that of the hot zone (where the combustion occurred), for each experiment carried out at the same preset temperature a temperature profile along the monolith was measured. In the initial series of experiments the ignition temperature of the combustion was determined as the highest monolith temperature for which (inde-

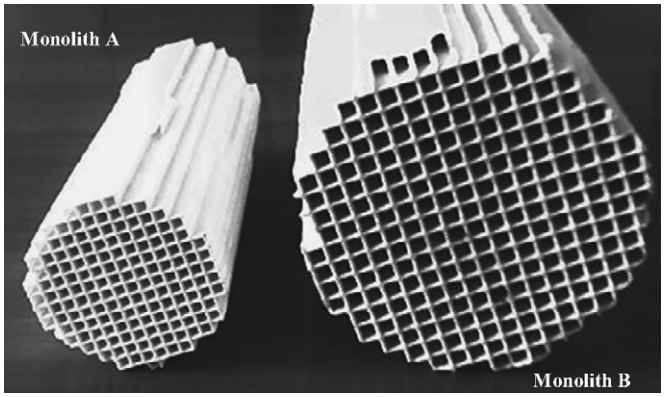

Fig. 7. Monoliths A and B.

Fig. 8. Experimental installation to study combustion over the monolith packing.

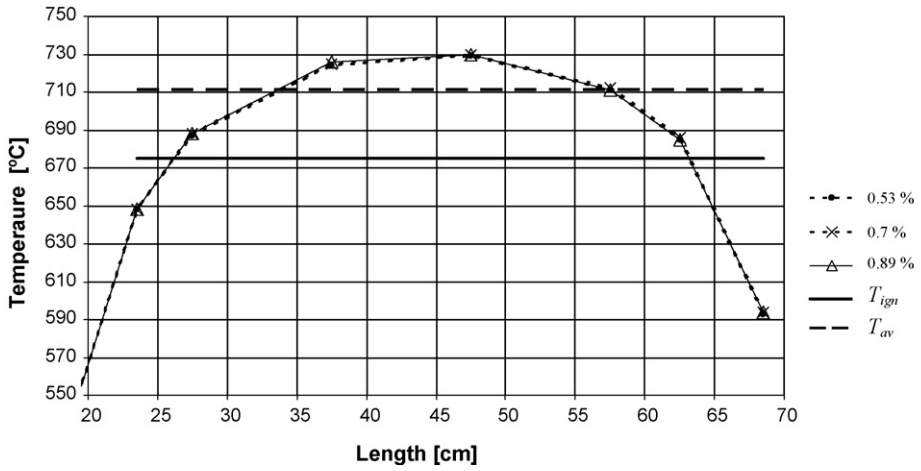

Fig. 9. An example of the temperature profiles along the monolith for the constant preset temperature of the oven and various inlet methane concentrations [vol.%] during kinetic experiments.

pendently of the inlet methane concentration) the combustion did not start (i.e., methane conversion was equal to zero). This temperature, T_{ign}, is shown in Fig. 9 as a solid line. As can be seen from Fig. 9, the temperature profiles are practically independent of methane concentration.

It is even difficult to differentiate between the individual profiles for different concentrations. The ignition temperature line makes it possible to determine the length of the combustion zone, L_{comb}, in the monolith, i.e., a part of the monolith where the combustion can appear. For the case shown in Fig. 9 this zone was estimated roughly as $L_{comb} \approx 37$ cm. Obviously, the higher the preset temperature in the oven, the longer the "combustion zone". As the temperature of the homogeneous combustion an average temperature T_{av} in the combustion zone was calculated, and this value was taken as a basis for the determination of a single point in the Arrhenius plot (shown in Fig. 10 for the oxidation of methane to carbon monoxide (2) and for the consecutive–parallel scheme).

In contrast to the experiments done over Monolith A, for Monolith B (similarly as for the free-space system) carbon monoxide was detected in the reaction products. The amount of CO depended on temperature. The conversions of methane towards the individual products are shown in Fig. 11.

Similarly as for the free-space combustion, for Monolith B the kinetic constants were estimated separately for the three mechanisms (consecutive, parallel and consecutive–parallel). The values

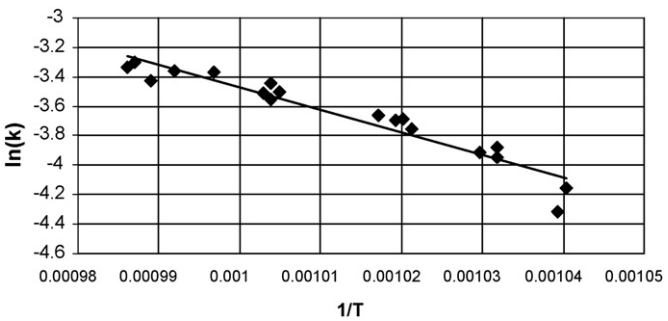

Fig. 10. The Arrhenius plot for the consecutive–parallel scheme-conversion of methane to carbon monoxide.

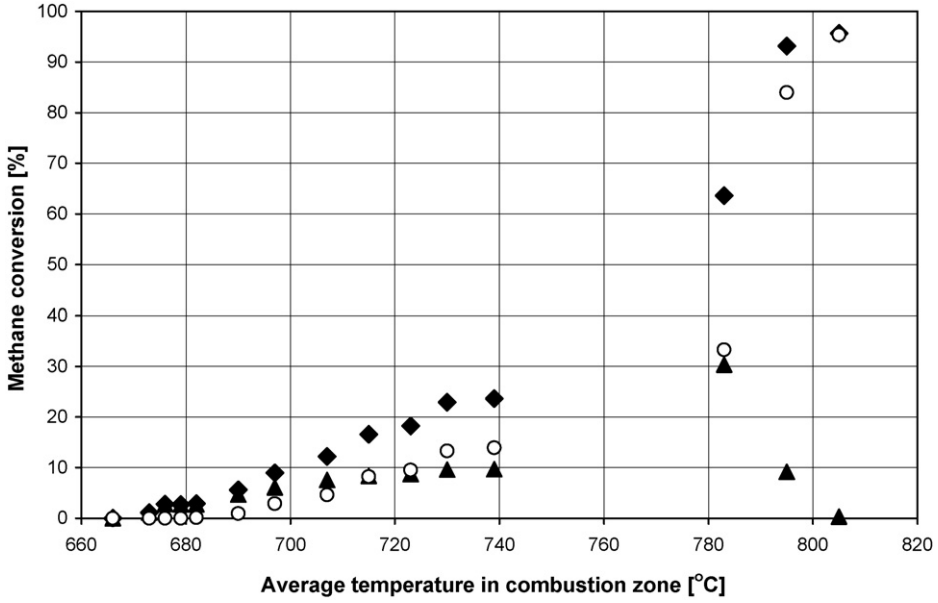

Fig. 11. Average conversions of methane: total (♦ α_{CH_4}), to carbon monoxide (▲ $\alpha_{CH_4/CO}$) and to carbon dioxide (○ α_{CH_4/CO_2}) vs. average temperature in combustion zone.

of the activation energy and pre-exponential factor are shown in Table 3. The quality of the kinetic equations thus obtained was assessed based on the average relative error of the reaction rate. The error was calculated using the following equations:

$$\Delta_r = \frac{1}{n}\sum_{k=1}^{n}\frac{|r_k^{meas} - r_k^{calc}|}{r_k^{meas}} \times 100\% \quad (9)$$

$$\Delta_c = \frac{1}{n}\sum_{k=1}^{n}\frac{|C_{p,k}^{meas} - C_{p,k}^{calc}|}{C_{p,k}^{meas}} \times 100\% \quad (10)$$

The values of the errors shown in Table 3 were evaluated only for such a range of temperatures for which methane conversion was less than 25%. For this range, the amount of CO produced in the system was comparable with that of CO_2. In some cases (for the parallel scheme) the error of estimation drastically increases at higher temperatures, when CO content becomes close to zero. Therefore, a relatively small estimation error in Table 3 does not necessarily mean an enhanced practical usefulness of the corresponding kinetic equation. We have to remember that formulae similar to Eq. (4) are unable yield reasonable simulation results in the range of temperatures over which the rate of CO formation drops (cf. Fig. 11). Consequently, the parallel scheme should be discarded in analyzing the results obtained. However, we can still try to determine the kinetic parameters for this scheme, provided a formula different from Eq. (4) is used for the rate of oxidation to CO. The consecutive scheme can be rejected due to the errors larger than those for the consecutive–parallel mechanism (over the range of temperatures for which the kinetics was determined for this scheme). Finally, for Monolith B the consecutive–parallel scheme seems to describe best methane oxidation to both CO_2 and CO.

6. Conclusions

The kinetic results obtained for the combustion of lean methane–air mixtures in three different systems (free space, Monolith A and Monolith B) clearly reveal a strong dependence of the kinetics of the oxidation upon the type of the experimental system. They also show that the surface area available for the gas phase may play an important role in activating and deactivating free radicals, and thus alter reaction mechanisms and affect both the combustion kinetics and intermediate products. The widely divergent results for Monolith A and B (which differ in geometric surface area (GSA) by around 330 m^2/m^3) suggest some form of pseudo-catalytic influence of the monolith walls on the homogeneous combustion of methane. The detailed conclusions may be summarized as follows:

(a) The ignition temperature for the homogeneous combustion of methane strongly depends on the area of the surface in contact with the gas phase. The lower the surface area, the higher the ignition temperature. For Monolith A, characterized by relatively narrow channels, this temperature was about 300 °C lower than for the oxidation in the free-space system.
(b) A simplified kinetic model should allow for the formation of carbon monoxide as an intermediate product, since under certain conditions (free space or Monolith B with wide channels) considerable amounts of CO may temporarily form at lower temperatures.
(c) If the parallel scheme is assumed (Eqs. (4) and (5)), the kinetic model may generate terms close to the indeterminate form ($\infty \times 0$), and thus lead to excessive errors in numerical calculations. From the physical standpoint, for higher teperatures, such a model can simulate the situation in which CO_2 is the final product not accompanied by CO in only one way: by discarding the oxidation of CH_4 to CO altogether (reaction (2)) and substituting the single-stage model for the two-stage scheme, with the complete combustion of methane according to reaction (1). For the two-stage mechanism this type of kinetics should not be taken into consideration.
(d) The consecutive–parallel scheme seems to be the most flexible. This scheme allows for both direct combustion of methane in accordance with reaction (1) and the consecutive oxidation via reactions (2) and (3). However, in the case of combustion in the free space this mechanism also yields a kinetic equation close to the indeterminate form ($\infty \times 0$), and the consecutive scheme may thus prove superior.
(e) If the formation of carbon monoxide is not found experimentally (combustion in small narrow channels Monolith A), the single-stage mechanism (reaction (1)) is sufficiently accurate.

Acknowledgements

This study was partly financed by the Polish Ministry of Science and Higher Education (grant No. R 14 020 02).

The monoliths used in the experiments were kindly supplied free of charge by the firm "Rauschert–Myslakowice". The authors gratefully acknowledge their assistance.

References

[1] M. De Joannon, P. Sabia, A. Tregrossi, A. Cavaliere, Dynamic behavior of methane oxidation in premixed flow reactor, Combust. Sci. Technol. 176 (2004) 769–783.
[2] K. Annamalai, I.K. Puri, Combustion Science and Engineering, CRC Press Taylor&Francis Group, 2007.
[3] P. Barbe, F. Battin-Leclerc, G.M. Come, Experimental and modeling study of methane and ethane oxidation between 773 and 1573 K, J. Chim. Phys. 92 (1995) 1666–1692.
[4] E. Ranzi, A. Sogaro, P. Gaffuri, G. Pennati, T. Faravelli, A wide range modeling study of methane oxidation, Combust. Sci. Technol. 96 (1994) 279–325.
[5] A.A. Slepterev, V.S. Salnikov, P.G. Tsyrulnikov, A.S. Noskov, V.N. Tomilov, N.A. Chumakova, A.N. Zagoruiko, Homogeneous high-temperature oxidation of methane, React. Kinet. Catal. Lett. 91 (2) (2007) 273–282.
[6] K. Gosiewski, K. Warmuzinski, M. Jaschik, M. Tanczyk, Kinetics of thermal combustion of lean methane–air mixtures in reverse flow reactors, Chem. Process Eng. 28 (2007) 335–345.
[7] K. Gosiewski, Y.S. Matros, K. Warmuzinski, M. Jaschik, M. Tanczyk, Homogeneous vs. catalytic combustion of lean methane–air mixtures in reverse-flow reactors, Chem. Eng. Sci. 63 (2008) 5010–5019.
[8] J. Warnatz, Combustion Chemistry, Springer Verlag, New York, 1984.
[9] W. Tsang, R.F. Hampson, Chemical kinetic data base for combustion chemistry. Part I. Methane and related compounds, J. Phys. Chem. Ref. Data 15 (1986) 1087–1097.
[10] W. Tsang, Chemical kinetic data base for combustion chemistry. Part 2. Methanol, J. Phys. Chem. Ref. Data 16 (1987) 471–508.
[11] P. Dagaut, J.C. Boettner, M. Cathonnet, Methane oxidation: experimental and kinetic modeling study, Combust. Sci. Technol. 77 (1991) 127–148.
[12] G.P. Smith, M. Frenklach, H. Wang, T. Bowman, D. Golden, W. Gardiner, V. Lissianski, R. Serauskas, Combust. Res. Bull. 81 (1994).
[13] J.C. Mackie, Partial oxidation of methane: the role of the gas-phase reactions, Catal. Rev. - Sci. Eng. 33 (1991) 169–240.
[14] T.B. Hunter, H. Wang, T.A. Litzinger, M. Frenklach, The oxidation of methane at elevated pressures: experiments and modeling, Combust. Flame 97 (1994) 201–224.
[15] K. Hanamura, R. Echigo, S. Zhdanok, Superadiabatic combustion in porous medium, Int. J. Heat Mass Transfer 36 (1993) 3201–3209.
[16] V.Y. Basevich, A.A. Belyaev, S.M. Frolov, Global kinetic mechanisms for simulation of turbulent reacting flows. Part 1 (in Russian), Russ. J. Phys. Chem. 17 (9) (1998) 117–129.
[17] K.V. Dobrego, N.N. Gnesdilov, S.H. Lee, H.K. Choi, Overall chemical kinetics model for partial oxidation of methane in inert porous media, Chem. Eng. J. 144 (2008) 79–87.
[18] K.V. Dobrego, I.M. Kozlov, V.V. Vasiliev, J.P. Martin, P. Gillon, Influence of fuel fraction gradient on triple flame velocity in plain and axis-symmetrical channels, Int. J. Heat Mass Transfer 51 (2008) 1962–1969.
[19] C.K. Westbrook, F.L. Dryer, Simplified reaction mechanisms for the oxidation of hydrocarbon fuel in flames, Combust. Sci. Technol. 27 (1981) 31–43.
[20] T.P. Coffee, A.J. Kotlar, M.S. Miler, The overall reaction concept in premixed laminar steady-state flames. 2.Initial temperatures and pressures, Combust. Flame 58 (1984) 59–67.
[21] T.P. Coffee, A.J. Kotlar, M.S. Miler, The overall reaction concept in premixed laminar steady-state flames. 1.Stoichiometries, Combust. Flame 54 (1983) 155–169.
[22] N. Peters, Numerical simulation of combustion phenomena, Lect. Notes Phys. 241 (1985) 90–109.